Proceedings

of the

XXVI Congreso de Ecuaciones Diferenciales y Aplicaciones
XVI Congreso de Matemática Aplicada

Gijón (Asturias), Spain

June 14-18, 2021

CEDYA CMA 2020 GIJÓN

SēMA
Sociedad Española de Matemática Aplicada

Universidad de Oviedo

Editors:
Rafael Gallego, Mariano Mateos

Universidad de Oviedo
Servicio de Publicaciones de la Universidad de Oviedo
Campus de Humanidades. Edificio de Servicios. 33011 Oviedo (Asturias)
Tel. 985 10 95 03 Fax 985 10 95 07
http: www.uniovi.es/publicaciones
servipub@uniovi.es

ISBN: 978-84-18482-21-2

Foreword

It is with great pleasure that we present the Proceedings of the 26th Congress of Differential Equations and Applications / 16th Congress of Applied Mathematics (XXVI CEDYA / XVI CMA), the biennial congress of the Spanish Society of Applied Mathematics S$\vec{e}$MA, which is held in Gijón, Spain from June 14 to June 18, 2021.

In this volume we gather the short papers sent by some of the almost three hundred and twenty communications presented in the conference. Abstracts of all those communications can be found in the abstract book of the congress. Moreover, full papers by invited lecturers will shortly appear in a special issue of the S$\vec{e}$MA Journal.

The first CEDYA was celebrated in 1978 in Madrid, and the first joint CEDYA / CMA took place in Málaga in 1989. Our congress focuses on different fields of applied mathematics: Dynamical Systems and Ordinary Differential Equations, Partial Differential Equations, Numerical Analysis and Simulation, Numerical Linear Algebra, Optimal Control and Inverse Problems and Applications of Mathematics to Industry, Social Sciences, and Biology. Communications in other related topics such as Scientific Computation, Approximation Theory, Discrete Mathematics and Mathematical Education are also common.

For the last few editions, the congress has been structured in mini-symposia. In Gijón, we will have eighteen minis-symposia, proposed by different researchers and groups, and also five thematic sessions organized by the local organizing committee to distribute the individual contributions. We will also have a poster session and ten invited lectures. Among all the mini-symposia, we want to highlight the one dedicated to the memory of our colleague Francisco Javier "Pancho" Sayas, which gathers two plenary lectures, thirty-six talks, and more than forty invited people that have expressed their wish to pay tribute to his figure and work.

This edition has been deeply marked by the COVID-19 pandemic. First scheduled for June 2020, we had to postpone it one year, and move to a hybrid format. Roughly half of the participants attended the conference online, while the other half came to Gijón. Taking a normal conference and moving to a hybrid format in one year has meant a lot of efforts from all the parties involved. Not only did we, as organizing committee, see how much of the work already done had to be undone and redone in a different way, but also the administration staff, the scientific committee, the mini-symposia organizers, and many of the contributors had to work overtime for the change.

Just to name a few of the problems that all of us faced: some of the already accepted mini-symposia and contributed talks had to be withdrawn for different reasons (mainly because of the lack of flexibility of the funding agencies); it became quite clear since the very first moment that, no matter how well things evolved, it would be nearly impossible for most international participants to come to Gijón; reservations with the hotels and contracts with the suppliers had to be cancelled; and there was a lot of uncertainty, and even anxiety could be said, until we were able to confirm that the face-to-face part of the congress could take place as planned.

On the other hand, in the new open call for scientific proposals, we had a nice surprise: many people that would have not been able to participate in the original congress were sending new ideas for mini-symposia, individual contributions and posters. This meant that the total number of communications was about twenty percent greater than the original one, with most of the new contributions sent by students.

There were almost one hundred and twenty students registered for this CEDYA / CMA. The hybrid format allows students to participate at very low expense for their funding agencies, and this gives them the opportunity to attend different conferences and get more merits. But this, which can be seen as an advantage, makes it harder for them to obtain a full conference experience. Alfréd Rényi said: "a mathematician is a device for turning coffee into theorems". Experience has taught us that a congress is the best place for a mathematician to have a lot of coffee. And coffee cannot be served online.

In Gijón, June 4, 2021

The Local Organizing Committee from the Universidad de Oviedo

Scientific Committee

- Juan Luis Vázquez, Universidad Autónoma de Madrid
- María Paz Calvo, Universidad de Valladolid
- Laura Grigori, INRIA Paris
- José Antonio Langa, Universidad de Sevilla
- Mikel Lezaun, Euskal Herriko Unibersitatea
- Peter Monk, University of Delaware
- Ira Neitzel, Universität Bonn
- JoséÁngel Rodríguez, Universidad de Oviedo
- Fernando de Terán, Universidad Carlos III de Madrid

Sponsors

- Sociedad Española de Matemática Aplicada
- Departamento de Matemáticas de la Universidad de Oviedo
- Escuela Politécnica de Ingeniería de Gijón
- Gijón Convention Bureau
- Ayuntamiento de Gijón

Local Organizing Committee from the Universidad de Oviedo

- Pedro Alonso Velázquez
- Rafael Gallego
- Mariano Mateos
- Omar Menéndez
- Virginia Selgas
- Marisa Serrano
- Jesús Suárez Pérez del Río

Contents

XXVI Congreso de Ecuaciones Diferenciales y Aplicaciones
XVI Congreso de Matemática Aplicada
Gijón, 14-18 junio 2021
(pp. 148–154)

FCF formulation of Einstein equations: local uniqueness and numerical accuracy and stability

Isabel Cordero-Carrión[1], **Samuel Santos-Pérez**[1], **Pablo Cerdá-Durán**[2]
1. *Departamento de Matemáticas, Universitat de València, E-46100 Burjassot, València, Spain.*
2. *Departamento de Astronomía y Astrofísica, Universitat de València, E-46100 Burjassot, València, Spain.*

Abstract

We present Einstein equations in the so-called Fully Constrained Formulation (FCF). This formulation has two different sectors: the elliptic sector formed by the Hamiltonian and Momentum constraints together with the equations derived from the gauge choice, and the hyperbolic sector which encodes the evolution of the rest of degrees of freedom of the spacetime metric including the gravitational waves. We present a modification of both sectors that keeps local uniqueness properties but has a better behaviour regarding the relativistic expansion of the equations. We also comment on numerical properties of this reformulation.

1. Introduction

Astrophysical scenarios containing compact objects are modeled by complex spacetimes which require, in general, to solve Einstein equations numerically. This is also true in the case of complex cosmological models. In the 3+1 decomposition of Einstein equations, spacetime is foliated through spacelike hypersurfaces. Doing this, the equations are decomposed in a set of elliptic equations, also called constraint equations, and a set of hyperbolic equations, also called evolution equations.

Constraint equations are only solved initially in the case of the approach by free evolution schemes. It is well known that if we evolve in time analytically some given initial data that satisfies the constraint equations using the evolution equations, then this data will also satisfy the constraint equations in posterior times, see [5]. This is true theoretically, but it may not be the case numerically. Formulations that solve the constraint equations on each time step are called constrained schemes. This work focuses on these schemes, and in particular in the so-called Fully Constrained Formulation (FCF) of the Einstein equations [2, 4].

This document is structured as follows. In Section 2 we introduce Einstein equations and the geometry of foliations. Section 3 describes technical details of a new reformulation of the FCF. In Section 4 we present the solution of the spacetime geometry of a neutron star considering the new reformulation of the FCF. We compare our solution with the one obtained with LORENE library, which employs spectral methods. We also make a comparison between our solution with the modification of the FCF equations and other approximate formulation that neglects the hyperbolic sector; this comparison confirms the accuracy improvement in the proposed reformulation of the FCF equations. Finally, in Section 5 we draw some conclusions and comment on future steps. From now on we use geometrical units in which $c = G = 1$, where c denotes the speed of light and G the universal constant of gravitation.

2. Einstein equations and foliations

Einstein Equations tells us how spacetime is curved according to the energy and matter content. These equations read

$$G_{\mu\nu} = 8\pi T_{\mu\nu}, \tag{2.1}$$

where $G_{\mu\nu}$ is the Einstein tensor, representing the information about the geometry of spacetime, and $T_{\mu\nu}$ is the energy-momentum tensor, concerning the distribution of energy and momentum. Einstein equations are a set of 10 non-linear coupled partial differential equations. They have exact solution only in a very few special cases, mostly in presence of symmetries. In general, they need to be solved numerically and this is the goal of Numerical Relativity.

Globally hyperbolic spacetimes allow to chose coordinates (t, x^i) such that level sets t = constant are spacelike hypersurfaces, that is, every tangent vector of these hypersurfaces is spacelike. Spacetime is thus foliated through spacelike hypersurfaces. The normal vector to these hypersurfaces is associated with the so-called Eulerian observer.

One important variable in Numerical Relativity is the lapse function $N(t, x^i)$, which is the factor connecting the lapse of proper time τ of this observer and the lapse of coordinate time t:

$$d\tau = N(t, x^i)dt. \tag{2.2}$$

Another important variable is the shift vector $\beta(t, x^i)$, which can be seen as the velocity between the Eulerian observer and the curves x^i = constant:

$$x^i_{t+dt} = x^i_{dt} - \beta^i(t, x^i)dt. \tag{2.3}$$

As the curves x^i = constant are not associated with any observer in general, the shift vector can be superluminical. This does not represent any physical propagation velocity, but just a foliation choice. The metric tensor of spacetime can be expressed as

$$g_{\mu\nu}dx^\mu dx^\nu = -N^2dt^2 + \gamma^{ij}(dx^i + \beta^i)(dx^j + \beta^j dt), \tag{2.4}$$

where γ^{ij} is the 3-metric in each hypersurface t = constant, also called the spatial metric. Therefore, Einstein equations can be decomposed in a set of evolution equations that have a hyperbolic character, and another set of constraint equations with elliptic character which have to be satisfied in each hypersurface and only depend on the spatial coordinates x^i.

3. Fully Constrained Formalism

The next manipulations are motivated by previous works and ideas described in [5]. First, we introduce a time independent flat background metric f_{ij}, which coincides with γ_{ij} at spatial infinity, and the following conformal decomposition:

$$\gamma^{ij} = \psi^4\tilde{\gamma}^{ij}. \tag{3.1}$$

We call γ_{ij} the conformal metric and $\psi := (\gamma/f)^{1/12}$ is the conformal factor, where $\gamma = \det \gamma_{ij}$ and $f = \det f_{ij}$. Let us denote by K^{ij} the extrinsic curvature on each hypersurface. We define the tensor A^{ij} as the traceless part of K^{ij}:

$$A^{ij} = K^{ij} - \frac{1}{3}K\gamma^{ij}, \tag{3.2}$$

where K represents the trace of extrinsic curvature. We also define $h^{ij} = \tilde{\gamma}^{ij} - f^{ij}$. Moreover, the gauge freedom of Einstein equations allow us to impose 4 extra conditions. In our case these will be $K = 0$ and

$$\mathcal{D}_k\tilde{\gamma}^{ki} = 0, \tag{3.3}$$

where $\mathcal{D}$ is the Levi-Civita connection associated with f^{ij}. The first condition is called maximal slicing and the second one generalized Dirac gauge. The next step is introducing a conformal decomposition of the extrinsic curvature,

$$K^{ij} = \psi^{10}\hat{A}^{ij}, \tag{3.4}$$

and at the same time its longitudinal/transverse decomposition,

$$\hat{A}^{ij} = (LX)^{ij} + \hat{A}^{ij}_{TT}, \tag{3.5}$$

introducing in this way the vector field X^i and the traceless and transverse tensor $\hat{A}^{ij}_{TT}$, $\mathcal{D}_i\hat{A}^{ij}_{TT} = 0$. L is the Killing operator. These last two definitions are motivated by the resolution of local uniqueness issues as it can be checked in [3].

Finally, we introduce two new fields

$$\dot{X}^i = \partial_t X^i,$$
$$V^i = 2N\psi^{-6}X^i - \beta^i,$$

in order to fix accuracy issues as we will discuss later on. These last two variables are introduced originally in this work. The following projections of the energy-momentum tensor are introduced for completeness,

$$S_{ij} = T_{\mu\nu}\gamma^\mu_i\gamma^\nu_j,$$
$$S^i = -\gamma^{i\mu}T_{\mu\nu}n^\nu,$$
$$S = \gamma^{ij}S_{ij},$$
$$E = T_{\mu\nu}n^\mu n^\nu,$$

and also the rescaled quantities $S_i^* = \psi^6 S_i$, $S^* = \psi^6 S$ and $E^* = \psi^6 E$. After all these definitions, we end up with an evolution equation for h^{ij},

$$\begin{aligned}\partial_t h^{ij} &= \beta^k \mathcal{D}_k h^{ij} - h^{ik}\mathcal{D}_k\beta^j - h^{kj}\mathcal{D}_k\beta^i + \frac{2}{3}h^{ij}\mathcal{D}_k\beta^k \\ &+2N\psi^{-6}\hat{A}^{ij}_{TT} + (LV)^{ij} - X^j\mathcal{D}^i(2N\psi^{-6}) - X^i\mathcal{D}^j(2N\psi^{-6}) + \frac{2}{3}f^{ij}X^k\mathcal{D}_k(2N\psi^{-6}),\end{aligned} \tag{3.6}$$

and another one for $\hat{A}^{ij}_{TT}$,

$$\begin{aligned}\partial_t \hat{A}^{ij}_{TT} &= \mathcal{D}_k\left(\beta^k\hat{A}^{ij}\right) - \hat{A}^{kj}\mathcal{D}_k\beta^i - \hat{A}^{ik}\mathcal{D}_k\beta^j + \frac{2}{3}\hat{A}^{ij}\mathcal{D}_k\beta^k + 2N\psi^{-6}\tilde{\gamma}_{kl}\hat{A}^{ik}\hat{A}^{jl} \\ &+\frac{3}{4}N\psi^{-6}\tilde{\gamma}^{ij}\tilde{\gamma}_{lk}\tilde{\gamma}_{nm}\hat{A}^{km}\hat{A}^{ln} + N\psi^2\tilde{R}^{ij}_* - \frac{1}{4}N\psi^2\tilde{R}\tilde{\gamma}^{ij} - \frac{1}{2}(\tilde{\gamma}^{ik}\mathcal{D}_k h^{lj} + \tilde{\gamma}^{kj}\mathcal{D}_k h^{il})\mathcal{D}_l(N\psi^2) \\ &+\mathcal{D}_k\left(\frac{N\psi^2}{2}\right)\tilde{\gamma}^{kl}\mathcal{D}_l h^{ij} - 8\pi N\psi^{10}S^{ij} + 4\pi N S^*\tilde{\gamma}^{ij} \\ &-(L\dot{X})^{ij} + 4\tilde{\gamma}^{ik}\tilde{\gamma}^{jl}\mathcal{D}_k\psi\mathcal{D}_l(N\psi) + 4\tilde{\gamma}^{ik}\tilde{\gamma}^{jl}\mathcal{D}_l\psi\mathcal{D}_k(N\psi) - 2\tilde{\gamma}^{ij}\tilde{\gamma}^{kl}\mathcal{D}_k\psi\mathcal{D}_l(N\psi) \\ &+\frac{N\psi^2}{2}\tilde{\gamma}^{kl}\mathcal{D}_k\left(\mathcal{D}_l h^{ij}\right) - \tilde{\gamma}^{ik}\tilde{\gamma}^{jl}\mathcal{D}_k\mathcal{D}_l(N\psi^2),\end{aligned} \tag{3.7}$$

where

$$\begin{aligned}\tilde{R}^{ij}_* = \frac{1}{2}\Big(&-\mathcal{D}_l h^{ik}\mathcal{D}_k h^{jl} - \tilde{\gamma}_{kl}\tilde{\gamma}^{mn}\mathcal{D}_m h^{ik}\mathcal{D}_n h^{jl} + \tilde{\gamma}_{nl}\mathcal{D}_k h^{mn}(\tilde{\gamma}^{ik}\mathcal{D}_m h^{jl} + \tilde{\gamma}^{jk}\mathcal{D}_m h^{il})\Big) \\ &+\frac{1}{4}\tilde{\gamma}^{ik}\tilde{\gamma}^{jl}\mathcal{D}_k h^{mn}\mathcal{D}_l\tilde{\gamma}_{mn},\end{aligned}$$

and

$$\tilde{R} = \frac{1}{4}\tilde{\gamma}^{kl}\mathcal{D}_k h^{mn}\mathcal{D}_l\tilde{\gamma}_{mn} - \frac{1}{2}\tilde{\gamma}^{kl}\mathcal{D}_k h^{mn} D_n\tilde{\gamma}_{ml}.$$

There is an issue concerning the post-newtonian order of the variables appearing in these equations. This means to expand variables in powers of $1/c$ in the approximation of low gravity and low velocity of the sources. These orders can be decuded from [1]. For instance, in equation (3.6) $\partial_t h^{ij}$ has leading post-newtonian order of $1/c^5$ which matches with the right hand side post-newtonian order. This is thanks to the introduction of the vector field V^i. If this were not the case, cancellations on the lower-order side must happen theoretically but it may not be the case numerically. A previous expression of (3.6) in [3], undergoes this problem as well as the equation (3.7): the left hand side has order $1/c^6$, meanwhile the terms of the last two lines of the right hand side of this equation have order $1/c^4$. This order correction is still a work in progress, but we already reduced the numbers of terms that should cancel analytically to get a lower order of $1/c^6$.

The constraint equations are the ones from the original elliptic sector of the FCF equations with some modifications and simplifications by the use of the vector field V^i, and additional elliptic equations for the variables $V^i, \dot{X}^i$. The whole elliptic sector is presented hereinafter (the post-newtonian order is placed beside each equation):

$$\Delta X^i + \frac{1}{3}\mathcal{D}^i\mathcal{D}_j X^j = -\tilde{\gamma}^{im}\left(\mathcal{D}_k\tilde{\gamma}_{ml} - \frac{1}{2}\mathcal{D}_m\tilde{\gamma}_{kl}\right)\hat{A}^{kl} + 8\pi\tilde{\gamma}^{ij}(S^*)_j = O\left(\frac{1}{c^3}\right); \tag{3.8}$$

$$\tilde{\gamma}^{kl}\mathcal{D}_k\mathcal{D}_l\psi = -2\pi\psi^{-1}E^* - \frac{1}{8}\psi^{-7}\tilde{\gamma}_{il}\tilde{\gamma}_{jm}\hat{A}^{lm}\hat{A}^{ij} + \frac{1}{8}\psi\tilde{R} = O\left(\frac{1}{c^2}\right); \tag{3.9}$$

$$\begin{aligned}\tilde{\gamma}^{ik}\mathcal{D}_i\mathcal{D}_k(N\psi^2) &= 2\psi^{-1}\tilde{\gamma}^{ik}\mathcal{D}_k\psi\mathcal{D}_i(N\psi^2) - 2\psi^{-2}(N\psi^2)\tilde{\gamma}^{ik}\mathcal{D}_k\psi\mathcal{D}_i\psi + \frac{3}{4}\psi^{-8}(N\psi^2)\tilde{\gamma}_{il}\tilde{\gamma}_{jm}\hat{A}^{lm}\hat{A}^{ij} \\ &+\frac{1}{4}(N\psi^2)\tilde{R} + 4\pi\psi^{-2}(N\psi^2)S^* = O\left(\frac{1}{c^4}\right);\end{aligned} \tag{3.10}$$

$$\begin{aligned}\Delta V^i + \frac{1}{3}\mathcal{D}^i\mathcal{D}_j V^j &= -h^{kl}\mathcal{D}_k\mathcal{D}_l V^i - \frac{1}{3}h^{ik}\mathcal{D}_k\mathcal{D}_j V^j + 2N\psi^{-6}\left(h^{kl}\mathcal{D}_k\mathcal{D}_l X^i + \frac{1}{3}h^{ik}\mathcal{D}_k\mathcal{D}_l X^l\right) \\ \mathcal{D}_k\mathcal{D}_l(2N\psi^{-6})\left(\tilde{\gamma}^{kl}X^i + \frac{1}{3}\tilde{\gamma}^{ik}X^l\right) &+ \mathcal{D}_k(2N\psi^{-6})\left(2\tilde{\gamma}^{kl}\mathcal{D}_k X^i + \frac{1}{3}\tilde{\gamma}^{ik}\mathcal{D}_l X^l + \frac{1}{3}\tilde{\gamma}^{ij}\mathcal{D}_j X^k - \hat{A}^{ik}\right) = O\left(\frac{1}{c^5}\right);\end{aligned} \tag{3.11}$$

$$
\begin{aligned}
&\Delta\dot{X}^j + \frac{1}{3}\mathcal{D}^j\mathcal{D}_i\dot{X}^i = \\
&\beta^k\mathcal{D}_i\mathcal{D}_k\hat{A}^{ij} - \mathcal{D}_i\hat{A}^{ik}\mathcal{D}_k\beta^j - \hat{A}^{ik}\mathcal{D}_i\mathcal{D}_k\beta^j + \frac{2}{3}\hat{A}^{ij}\mathcal{D}_i\mathcal{D}_k\beta^k + \frac{5}{3}\mathcal{D}_i\hat{A}^{ij}\mathcal{D}_k\beta^k \\
&-\frac{1}{2}N\psi^{-6}\tilde{\gamma}^{jl}\mathcal{D}_l\left(\tilde{\gamma}_{in}\tilde{\gamma}_{km}\hat{A}^{nm}\hat{A}^{ik}\right) - \psi^{-8}\tilde{\gamma}^{jl}\tilde{\gamma}_{in}\tilde{\gamma}_{km}\hat{A}^{nm}\hat{A}^{ik}\mathcal{D}_l(N\psi^2) + 8\psi^{-7}N\tilde{\gamma}^{jl}\tilde{\gamma}_{in}\tilde{\gamma}_{km}\hat{A}^{nm}\hat{A}^{ik}\mathcal{D}_l\psi \\
&+2N\psi^{-6}\mathcal{D}_i(\tilde{\gamma}_{kl}\hat{A}^{ik}\hat{A}^{jl}) - 16\psi^{-7}N\tilde{\gamma}_{kl}\hat{A}^{ik}\hat{A}^{jl}\mathcal{D}_l\psi + 2\psi^{-8}\tilde{\gamma}_{kl}\hat{A}^{ik}\hat{A}^{jl}\mathcal{D}_l(N\psi^2) \\
&-\frac{1}{2}\mathcal{D}_i(N\psi^2)\mathcal{D}_l h^{ik}\mathcal{D}_k h^{jl} - \frac{1}{6}\tilde{\gamma}^{kj}\mathcal{D}_k h^{il}\mathcal{D}_i\mathcal{D}_l(N\psi^2) - \tilde{\gamma}^{ik}\mathcal{D}_i h^{jl}\mathcal{D}_k\mathcal{D}_l(N\psi^2) \\
&-8N\tilde{\gamma}^{ik}\mathcal{D}_i h^{jl}\mathcal{D}_k\psi\mathcal{D}_l\psi + 4N\tilde{\gamma}^{jl}\mathcal{D}_l h^{ik}\mathcal{D}_i\psi\mathcal{D}_k\psi + 4\psi^{-1}\tilde{\gamma}^{ik}\mathcal{D}_i h^{jl}\left(\mathcal{D}_l(N\psi^2)\mathcal{D}_k\psi + \mathcal{D}_k(N\psi^2)\mathcal{D}_l\psi\right) \\
&-4\psi^{-1}\tilde{\gamma}^{jl}\mathcal{D}_l h^{ik}\mathcal{D}_i(N\psi^2)\mathcal{D}_k\psi + \tilde{R}^{ij}_{**}\mathcal{D}_i(N\psi^2) + N\psi^2\mathcal{D}_i\tilde{R}^{ij}_{**} - \frac{1}{2}N\psi^2\tilde{\gamma}^{ij}\mathcal{D}_i\tilde{R} \\
&-8\pi\psi^{-2}E^*\tilde{\gamma}^{jl}\mathcal{D}_l(N\psi^2) + 16\pi\psi^{-1}NE^*\tilde{\gamma}^{jl}\mathcal{D}_l\psi + 16\pi\psi^{-1}NS^*\tilde{\gamma}^{jl}D_l\psi \\
&-8\pi N\psi^{10}\mathcal{D}_i S^{ij} - 8\pi\psi^8 S^{ij}\mathcal{D}_i(N\psi^2) - 64\pi\psi^9 NS^{ij}\mathcal{D}_i\psi = O\left(\frac{1}{c^4}\right),
\end{aligned}
\tag{3.12}
$$

where

$$
\tilde{R}^{ij}_{**} = \frac{1}{2}\left(-\tilde{\gamma}_{kl}\tilde{\gamma}^{mn}\mathcal{D}_m h^{ik}\mathcal{D}_n h^{jl} + \tilde{\gamma}_{nl}\mathcal{D}_k h^{mn}(\tilde{\gamma}^{ik}\mathcal{D}_m h^{jl} + \tilde{\gamma}^{jk}\mathcal{D}_m h^{il})\right) + \frac{1}{4}\tilde{\gamma}^{ik}\tilde{\gamma}^{jl}\mathcal{D}_k h^{mn}\mathcal{D}_l\tilde{\gamma}_{mn}.
$$

We can see how the elliptic sector can be solved hierarchically and this sector now is decoupled in equations including terms with progressively lower post-newtonian orders: note that in equation (3.10) we solve $N\psi^2$ as we find that it has post-newtonian order $1/c^4$ instead of $1/c^2$ as N, see [1].

In the next Section we present the first tests of the proposed modified equations in this formulation by solving the spacetime geometry of a neutron star.

4. Results and discussion

In the following we set $h^{ij} = 0$ in such a way we can compare our results with the ones obtained with the xCFC formulation which imposes this condition, see [3], and can be seen as an approximation to the FCF. As a test we use a neutron star model with an equatorial radius of $R_e = 12.859$ km, central density $\rho_c = 7.91 \cdot 10^{14}$ g/cm^3 and angular velocity $\omega = 606$ rad/s. We consider that the star is composed of a perfect fluid with polytropic equation of state $p = C\rho^\Gamma$, where p is the pressure, $\Gamma = 2$ and $C = 145731$ (cgs units). For this compact object, spacetime is stationary and we can adapt the coordinate time t to this stationarity, setting the derivatives with respect to t in (3.6) and (3.7) to zero. Moreover, this spacetime is axisymmetric; we use spherical orthonormal coordinates adapting them to this axisymmetry and fixing the rotation axis at $\theta = 0$, being θ the polar angle in spherical orthonormal coordinates.

In order to compare elliptic sectors in both xCFC and modified FCF formulations, we will focus on this work on equations (3.8)–(3.12) regarding the modified FCF scheme. By using spherical orthonormal coordinates and considering axisymmetry, we just solve equations in the 2-dimensions. The mesh consist in 100 points in the radial coordinate r and 32 points in polar angle θ. We use one ghost cell to properly compute the discretization of derivatives close to the numerical domain boundaries. All discretizations of the differential operators are 2nd order and we use the LAPACK library to invert the Laplacian operators. In some equations the variable under resolution appears outside the main Laplacian operator in the source term; here we apply fix-point iterative methods with a relaxation factor.

Concerning boundary conditions, we apply periodicity in the polar angle θ and for the radial coordinate we set $u(r,\theta) = \pm u(r, \pi - \theta)$ for the inner boundary, where u represents a generic variable and the election of the sign depends on the symmetry of this variable. At the outer boundary we impose a Robin condition, assuming $u = u_0 + M/r^n$, which is equivalent to impose $\partial u/\partial r = -n(u - u_0)/r$, and only n and u_0 need to be specified. We have $n = 1$ for scalars fields and $n = 2$ for vector fields. u_0 is the asymptotic value of the variable at spatial infinity $r \longrightarrow \infty$.

In Figure 1 we show the results obtained for the numerical solutions of the variables X, ϕ and N. Only the angular component of X^i, X^ϕ, is non-zero. We plot the radial profile of these variables at $\theta = \pi/2$. Figure 2 shows the numerical solution of the new introduced vector field V^i, and the shift vector β^i directly computed from V^i. For this vector fields again only the angular components V^ϕ and β^ϕ are non-zero. We plot the radial profile of these variables at $\theta = \pi/2$.

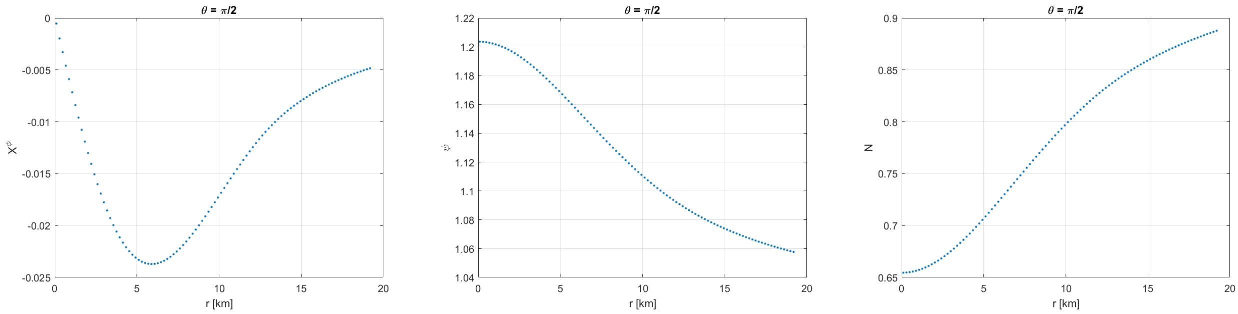

Fig. 1 Radial profiles of X^ϕ, the conformal factor ψ and the lapse function N at $\theta = \pi/2$.

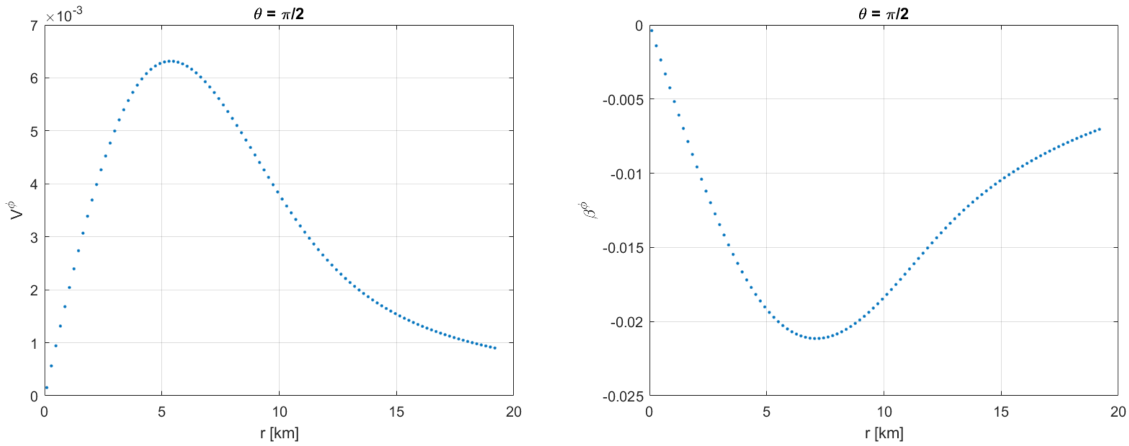

Fig. 2 Radial profiles of V^ϕ and third component of the shit vector β^ϕ at $\theta = \pi/2$.

Finally, the numerical solution for the other new vector field introduced $\dot{X}^i$ is shown in Figure 3. Here only the angular component, $\dot{X}^\phi$, is exactly equal to zero. Therefore, we plot the radial profile of $\dot{X}^r$ and $\dot{X}^\theta$ at $\theta = \pi/2$. This is the first time that the vector field $\dot{X}$ is computed numerically. Being a time derivative, it must be zero as our spacetime is stationary. Nevertheless, we get values different from zero due to the fact that the tensor h^{ij} has been neglected. In Figures 1– 3, the radial outer boundary is placed at 1.5 times the equatorial star radius R.

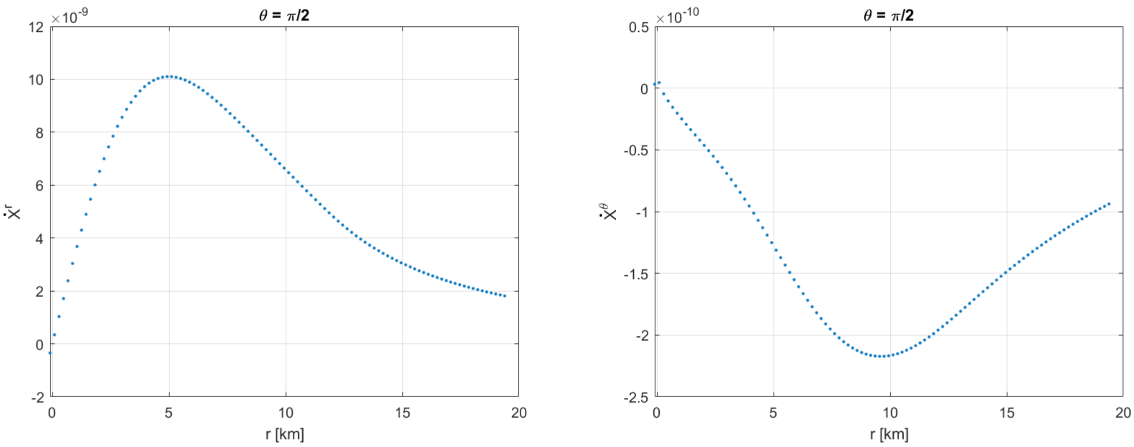

Fig. 3 Radial profiles of $\dot{X}^r$ and $\dot{X}^\theta$ at $\theta = \pi/2$.

A deeper analysis of the accuracy has been carried out by considering different resolutions in the radial coordinate as well as different locations of the outer boundary. Placing further the outer boundary, we expect to increase accuracy in the numerical solutions of our variables. This is expected since placing further the outer boundary translate into a closer tend to the main decay of the variables as $r \to \infty$, as we know that spacetime is asymptotically flat.

In other to numerically check the accuracy of our results, we compute the residuals as the comparison between the solution obtained with LORENE [6], and our numerical solutions; specifically,

$$\sigma(f) = \max |f - f_{\mathrm{LORENE}}|, \tag{4.1}$$

where f and f_{LORENE} are the numerical solutions computed by us and by LORENE, respectively.

Figure 4 shows the residuals of the lapse function N, the conformal factor and the shift vector in logarithmic scale in terms of the spatial radial resolution also in logarithmic scale, employing the xCFC and modified FCF equations. Each colour refers to a specific location of the outer boundary; for example, $B/R = 1.5$ means that the outer boundary has been placed at 1.5 times the equatorial coordinate radius of the neutron star, B would be the size of the radial grid.

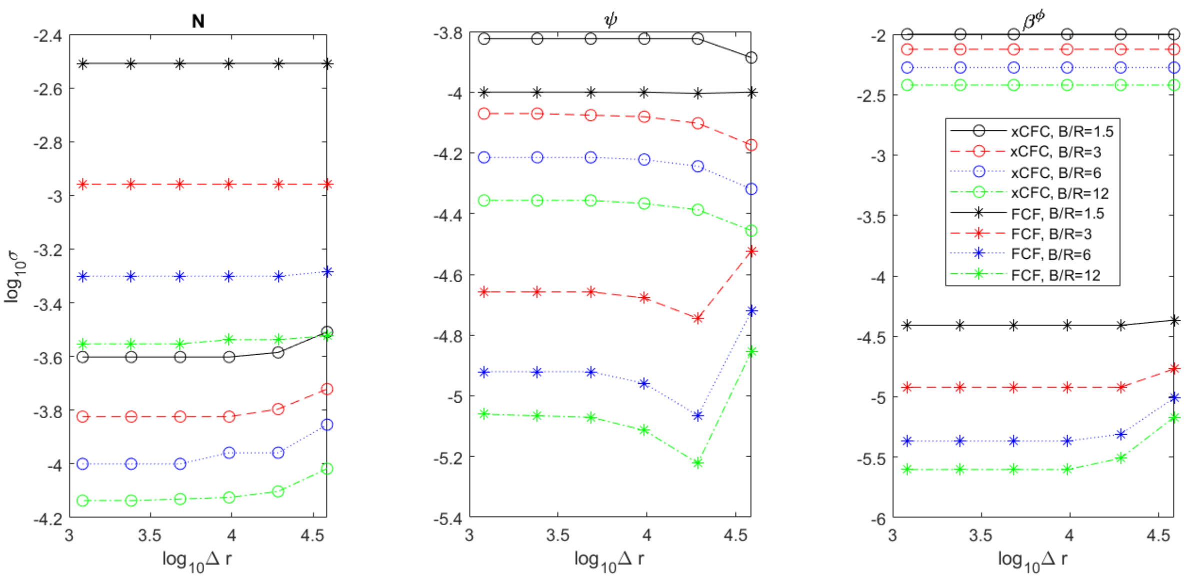

Fig. 4 Residuals of the the lapse function N (left), conformal factor ψ (center) and shift vector β^ϕ (right) versus the spatial resolution of the radial coordinate. Logarithmic scale is employed in both axis. Asterisks correspond to xCFC and circles to FCF. Each colour/line is linked with a grid size according to the common legend.

In all cases, the main reason to increase accuracy above a certain radial reasonable resolution is the location of the outer boundary for both the xCFC and the modified FCF equations: the further the outer boundary is located, the better the numerical accuracy for all the variables. This is a key point in the numerical resolution of the elliptic sector and we also expect to find a similar behavior for the numerical resolution of the hyperbolic sector in future works, taking into account that this hyperbolic sector encodes the gravitational radiation of the studied astrophysical scenario.

We lose some accuracy for the lapse function N in the modified FCF case, but this could be because we have to deal with a spatial derivative of the lapse function in the source terms. This fact does not happen in the xCFC case (see [3], to check the exact expressions in the elliptic sector for this formulation). The difference in the residuals decrease when increasing the radius of the location of the outer boundary and are expected to be comparable for good resolutions. We want to explore in more details the possibility of including the spatial derivative on the right hand side of (3.10) in the discretization of the elliptic operator on the left hand side, so checking weather the numerical accuracy of the lapse function can increase. When radial resolution is increased we observe a slightly improvement in the values of the residuals, but they cannot be noticed in Figures 4 due to the logarithmic scales of the vertical axis.

For the vector fields V^i and β^i, the numerical resolution of the modified FCF equations provide a much better accuracy. In the case of the shift vector β^i we gain around two orders of magnitude. This is also quite reasonable since the introduction of the V^i vector is strongly related to the shift vector. We want to remind that for the xCFC case, an elliptic equation for the shift vector is solved, see [3], while in the modified FCF equations the vector V^i is solved and then the shift vector is computed directly from the vector V^i definition.

Going from the xCFC to the modified FCF equations, we also have the possibility of including non zero h^{ij} values in the source of the equations in the elliptic sector, thus getting better accuracy in the computation of our numerical variables. This is indeed the case for a rotating neutron star, where a conformally flat metric cannot reproduce the geometry of this spacetime. This is actually a step for future works: include non-zero values for h^{ij}, include the corresponding hyperbolic sector, and take into account these terms also in the sources of the equations of the elliptic sector.

Despite the lack of reduction of the post-newtonian orders of the source terms in equation (3.7), we can take advantage of the fact that these terms should be neglected up to $1/c^6$ order to get an estimate of the h^{ij} components, by solving the following elliptic equation:

$$(\Delta h)^{ij} = 2(N\psi^2)^{-1}\Big(8Nf^{ik}f^{jl}\mathcal{D}_l\psi\mathcal{D}_k\psi - 2Nf^{ij}f^{kl}\mathcal{D}_k\psi\mathcal{D}_l\psi + f^{ik}f^{jl}\mathcal{D}_k\mathcal{D}_l(N\psi^2) + (L\dot{X})^{ij} + 8\pi N\psi^{10}S^{ij} - 4\pi NS^* f^{ij}\Big).$$

This point should be further analyzed in next works to check if a better proposal can be obtained. Moreover, we also want to numerically solve these equations and check our results.

5. Conclusions

We have been accomplished the first step towards a Fully Relativistic Formulation in the Fully Constrained Formalism. Constrained formulations allow to carry out long term simulations without constraint equations violations. Besides, it posses the properties of local uniqueness, hierarchical resolutions and correct relativistic expansion with the exception of those terms mentioned in equation (3.7).

It remains for the future to check accuracy in complex numerical simulations, as well as include the hyperbolic sector of the evolution equations. This has huge impact in the calibration of gravitational waves templates. Another possible project would be to use leading terms in simplified numerical simulations for cosmological applications, e.g., to compute gravitational waves estimates in cosmological contexts, where requirements of being far away from the source (as in the famous quadrupole formula) do not apply.

References

[1] L. Blanchet, T. Damour & G. Schäefer. Post-Newtonian hydrodynamics and post-Newtonian gravitational wave generation for numerical relativity. Monthly Notices of the Royal Astronomical Society ;242(3):289-305, 1990.

[2] S. Bonazzola, E. Gourgoulhon, P. Grandclément & J. Novak. Constrained scheme for the Einstein equations based on the Dirac gauge and spherical coordinates, Physical Review D 70, 104007, 2004

[3] I. Cordero-Carrión, P. Cerdá-Durán, H. Dimmelmeier, J. L. Jaramillo, J. Novak & E. Gourgoulhon. Improved constrained scheme for the Einstein equations: An approach to the uniqueness issue. Physical Review D, 79(2), 024017, 2009

[4] I. Cordero-Carrión, J.M. Ibáñez, E. Gourgoulhon, J.L. Jaramillo & J. Novak. Mathematical issues in a fully constrained formulation of the Einstein equations. Physical Review D 77, 084007, 2008.

[5] E. Gourgoulhon. 3+1 formalism in general relativity: bases of numerical relativity (Vol. 846). Springer Science & Business Media, 2012.

[6] http://www.lorene.obspm.fr/.